

2009

Cyclic Voltammetry of Biofilms of Wild Type and Mutant *Geobacter Sulfurreducens* on Fuel Cell Anodes Indicates Possible Roles of OmcB, OmcZ, type IV Pili, and Protons in Extracellular Electron Transfer

Derek Lovley, *University of Massachusetts - Amherst*

Hanno Richter

Kelly P Nevin

Hongfei Jia

Daniel A Lowy, et al.

Cyclic voltammetry of biofilms of wild type and mutant *Geobacter sulfurreducens* on fuel cell anodes indicates possible roles of OmcB, OmcZ, type IV pili, and protons in extracellular electron transfer†

Hanno Richter,^a Kelly P. Nevin,^a Hongfei Jia,^b Daniel A. Lowy,^c Derek R. Lovley^a and Leonard M. Tender^{*d}

Received 23rd September 2008, Accepted 8th January 2009

First published as an Advance Article on the web 4th February 2009

DOI: 10.1039/b816647a

Geobacteraceae are distinct for their ability to reduce insoluble oxidants including minerals and electrodes without apparent reliance on soluble extracellular electron transfer (ET) mediators. This property makes them important anode catalysts in new generation microbial fuel cells (MFCs) because it obviates the need to replenish ET mediators otherwise necessary to sustain power. Here we report cyclic voltammetry (CV) of biofilms of wild type (WT) and mutant *G. sulfurreducens* strains grown on graphite cloth anodes acting as electron acceptors with acetate as the electron donor. Our analysis indicates that WT biofilms contain a conductive network of bound ET mediators in which OmcZ (outer membrane *c*-type cytochrome Z) participates in homogeneous ET (through the biofilm bulk) while OmcB mediates heterogeneous ET (across the biofilm/electrode interface); that type IV pili are important in both reactions; that OmcS plays a secondary role in homogenous ET; that OmcE, important in Fe(III) oxide reduction, is not involved in either reaction; that catalytic current is limited overall by the rate of microbial uptake of acetate; that protons generated from acetate oxidation act as charge compensating ions in homogenous ET; and that homogenous ET, when accelerated by fast voltammetric scan rates, is limited by diffusion of protons within the biofilm. These results provide the first direct electrochemical evidence substantiating utilization of bound ET mediators by *Geobacter* biofilms and the distinct roles of OmcB and OmcZ in the extracellular ET properties of anode-reducing *G. sulfurreducens*.

Introduction

In microbial fuel cells (MFCs) microorganisms catalyze the anode half-reaction by metabolizing fuel and utilizing the anode as an electron acceptor.¹ MFCs combine the wide range of biomass-derived fuels with long-term durability of microbial

consortia. While the underlying concept has been known for decades,² only recently has a MFC been demonstrated as a practical alternative to conventional power sources for specific applications.³ While many microorganisms have been utilized in MFCs²⁻⁵ our studies have focused on *Geobacter sulfurreducens* because it is closely related to the *Geobacteraceae* enriched in biofilms formed on anodes of MFCs harvesting electricity from a variety of aquatic sediments.⁶⁻⁸ In addition this organism is often enriched on anodes of MFCs designed to study their potential for wastewater treatment.⁹⁻¹² This enrichment may result from its ability to generate high current densities at high coulombic efficiencies without apparent reliance on soluble ET mediators,¹³⁻¹⁵ a desirable property for MFCs because it eliminates the need to maintain ET mediators (either endogenous, secreted by the organisms or exogenous, added externally) in the anodic half cell enabling uninterrupted power generation

^aDepartment of Microbiology, Morrill Science Center IV North, University of Massachusetts, Amherst, MA, 01003, USA

^bToyota Research Institute of North America, Ann Arbor, MI, 48105, USA

^cNova Research, Inc., 1900 Elkin St., Alexandria, VA, 22308, USA

^dCenter for Biomolecular Science and Engineering, Naval Research Laboratory, 4555 Overlook Ave., SW, Washington, DC, 20375, USA

† Author contributions: H. J., H. R., K. P. N., D. R. L., and L. M. T. designed research; H. R. and H. J. performed research; H. R., D. A. L., and L. M. T. analyzed data; H. R., D. R. L., and L. M. T. wrote the paper.

Broader context

Geobacteraceae are extensively studied for their significant environmental impact. They are distinct for their ability to exchange electrons with electrodes without apparent reliance on soluble extracellular electron transfer (ET) mediators, making them important anode catalysts in new generation microbial fuel cells because it obviates the need to replenish ET mediators otherwise necessary to sustain power. Here we provide the first description of the mechanism of electrode reduction by *Geobacteraceae*, determine probable roles played in this process by various proteins, and determine the rate limiting steps.

with continual addition of fuel. Furthermore, availability of its genome sequence and a genetic system makes it feasible to rationally investigate contributions of its cellular components to its power generation capabilities.^{16,17}

Significant investigation of extracellular ET by anode-bound biofilms of *G. sulfurreducens* has implicated various redox active outer membrane *c*-type cytochromes.^{14,16–37} In thin (*ca.* 10 μm thick) WT biofilms, genes for OmcS and OmcE are more highly expressed than in planktonic cells grown with a soluble electron acceptor such as Fe(III) citrate.¹⁶ In thick (*ca.* 50 μm) biofilms^{32,36} where homogenous ET is presumably more challenged, whole genome analysis of gene transcript abundance revealed genes more highly expressed in cells grown on electrodes maintained at oxidizing potentials (*i.e.*, anodes) than on identical non-potentiated electrodes (*i.e.*, at open circuit) with fumarate serving as the electron acceptor.³⁶ One such gene is for OmcB, known to be partially inserted in the outer membrane.³¹ OmcE is also up-regulated, whereas OmcS is down-regulated.³⁶ Simultaneous deletion of OmcB, OmcE, and OmcS temporarily inhibits electricity generation, and adaption by this strain is accompanied by increased abundance of OmcZ.³⁷ An additional up-regulated gene in thick biofilms is for PilA, the structural protein (not redox active) of type IV pili in *G. sulfurreducens*, found to be essential for Fe(III) oxide reduction.¹⁷ A strain, in which PilA is deleted, produces significantly less current than WT cells, and exhibits no adaptation to WT-level current production even after extended incubation.^{32,36} In addition, the gene for OmcZ exhibits a much higher transcript abundance in anode-grown than fumarate-grown biofilm cells, and deletion of this gene severely inhibits current production with no long-term adaption.³⁶

Using CV, Bond *et al.*³⁸ established the precedent that anode-bound *G. sulfurreducens* in biofilms, and entrapped in pectin exhibit electrochemical properties consistent with anode-bound catalysts. More recently, they used CV to electrochemically characterize anode-bound biofilms of *Shewanella*.³⁹ Their characterization revealed that *Shewanella oneidensis* MR-1 and *Shewanella sp.* MR-4 secrete riboflavin, which acts as a soluble extracellular ET mediator in extracellular ET from individual microbes in biofilms to the underlying anodes. CV of anode-bound *Shewanella* and *Geobacter* are markedly different^{38,39} reflecting possible fundamental differences in their extracellular ET properties. While previous studies indicate that *Shewanella* species can reduce insoluble electron acceptors, such as Fe(III) oxides or electrodes not in contact with the cells,^{8,14,24,40–44} *Geobacter* species must be in contact with insoluble electron acceptors in order to reduce them and investigations of the potential utilization of endogenous soluble ET mediators by *Geobacter* and related species have yielded only negative results.^{6,14,45}

CV is a time-honored electroanalytical technique, used extensively for studying charge transfer in electrochemical systems. In the context of electrode-bound catalysts, it is used to probe the mechanism of ET from substrate (*e.g.*, acetate) to the electrode surface by changing the driving force and rate of the heterogeneous ET step (across the catalyst/electrode interface) by means of changing the electrode potential (*E*). Monitoring current (*i*) as a function of *E* and rate of change of *E* (voltammetric scan rate, ν) yields *i*–*E*– ν dependencies that can provide detailed mechanistic information about the entire ET mechanism. Here we expand upon the use of CV by Bond *et al.*³⁸ to

investigate in greater detail anode-bound biofilms of *G. sulfurreducens*. We compare *i*–*E*– ν dependencies of WT to an OmcB-deletion mutant (ΔomcB), an OmcE-deletion mutant (ΔomcE), an OmcS deletion mutant (in which OmcT expression is inhibited (ΔomcST)), an OmcZ-deletion mutant (ΔomcZ), and a PilA-deletion mutant (ΔpilA), and determine possible roles of the above proteins in microbe-to-anode extracellular ET. We propose a multistep extracellular ET mechanism drawing on prior electrochemical investigations of electrode-bound catalysts, demonstrate that protons generated within the biofilm from microbial oxidation of acetate act as charge compensating ions, corroborate recent results that implicate the flux of these protons in limiting the rate of homogeneous ET in WT *G. sulfurreducens* biofilms⁴⁶ and provide direct electrochemical evidence substantiating use of bound ET mediators by an anode-bound biofilm.

Methods

Microbial fuel cells

MFCs were constructed from commercially available methanol fuel cells as described previously.¹⁵ Briefly, for each MFC, the volume of each half cell was 10 mL. Both the anode and cathode were comprised of graphite cloth (type GC-14, Electrolytica, Inc., Amherst, NY), separated by a Nafion® 117 membrane (3.5 cm \times 3.5 cm). The cathode and anode were connected by a 560 Ω resistor during biofilm growth. The anode and cathode electrical connections were fashioned as previously described.¹⁵ Dimensions of the cathode and anode were 2.54 cm \times 2.54 cm and 1.27 cm \times 0.64 cm, respectively. The anode surface area was estimated to be 2.40 cm² by comparing maximum catalytic current of biofilms on carbon cloth with that accomplished on plane graphite rod electrodes with known dimensions. This result was supported by calculations based on the diameter and thread count of the fibers comprising the carbon cloth anode. A Ag/AgCl, 3 M KCl reference electrode (BAS, West Lafayette, IN, USA) was positioned in the anodic half cell with the tip approximately 0.5 cm from the anode face. The anode and cathode half cells were supplied with sterile media (described below) using Masterflex PharMed BPT tubing and peristaltic pumps. All MFC components were sterilized and assembled as previously described.¹⁵

Organisms, media and growth conditions

Geobacter sulfurreducens strain PCA (ATCC 51573, DSMZ 12127⁴⁷) and mutants lacking PilA,¹⁷ OmcB,²⁶ OmcE,¹⁸ OmcST (ΔomcS since OmcT is also not expressed in the ΔomcS mutant¹⁸) and OmcZ³⁶ were obtained from an in-house culture collection. Each strain was cultured with 10 mM acetate and 40 mM fumarate in pressure tubes under strict anaerobic conditions in NBAF medium as previously described⁴⁸ and subsequently investigated in its own MFC. Cell growth in each MFC was performed as previously described¹⁵ but utilizing a freshwater medium⁴⁹ containing 0.06 g L⁻¹ NaH₂PO₄. Briefly, for each strain, 250 ml of sterile media containing a 10% culture inoculum, 10 mM acetate and 10 mM fumarate was re-circulated through the anodic half cell while the anode was electrically connected to the cathode by a 560 Ω resistor. Media containing only 50 mM K₃Fe(CN)₆. Once an optical density of 0.2 was achieved, 250 ml of sterile media lacking cells and fumarate, but

containing 10 mM acetate, was re-circulated through the anodic half cell at a dilution rate of 8.6 h⁻¹ to remove planktonic cells and fumarate from the half cell.

Analytical

During biofilm growth, the voltage across the 560 Ω resistor connecting the anode and cathode of each MFC was recorded hourly. Once a stable electrical current was achieved across the resistor (ca. 0.5 mA in the case of WT) indicating a fully grown biofilm, the resistor was removed and the anode maintained by potentiostat at 0.300 V vs. the Ag/AgCl reference electrode (0.500 V vs. the standard hydrogen electrode (SHE)) using the cathode as the auxiliary electrode and fresh sterile media lacking cells and fumarate but containing 10 mM acetate was continuously flowed through the anodic half cell at a dilution rate of 0.86 h⁻¹. During CV the media flow rate was increased to a dilution rate of 8.6 h⁻¹.

The potentiostat (Model 2053, AMEL Instruments, Milano, Italy) was operated by a Macintosh computer running software (Echem version 2.010, eDAQ, Colorado Springs, CO, USA) interfaced to the potentiostat with a Powerlab data acquisition system (Model 4SP, ADInstruments, Colorado Springs, CO, USA). CV was performed from +0.300 to -0.500 V vs. the Ag/AgCl reference electrode at scan rates from 0.002 to 5.000 V s⁻¹. All potentials are reported hereon vs. SHE by subtraction of 0.200 V for easier comparison to biological redox potentials. No real-time IR compensation was employed while recording CV. Post analysis of the CV depicted here based on the semi-integral method described by Bond *et al.*⁵⁰ yielded a value for the uncompensated solution resistance of 0.332 ± 0.070 Ω (*n* = 5), indicating a negligible IR loss of 0.0018 V at 5 V s⁻¹.

Confocal microscopy

Biofilms on graphite cloth electrodes were fluorescently stained with the LIVE/DEAD BacLight Bacterial Viability Kit (L7012, Molecular Probes, Inc., Eugene, OR, USA) and examined by confocal laser scanning microscopy, as previously described¹⁵ for determination of biofilm thickness.

Results and discussion

Growth of wild type and mutant biofilms on graphite anodes

Fig. 1 depicts typical current vs. time records during biofilm growth for WT *G. sulfurreducens* and the five mutants ($\Delta omcB$,

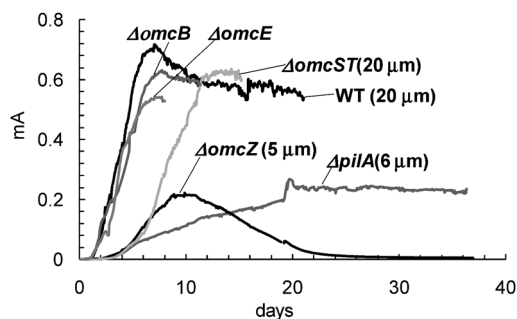
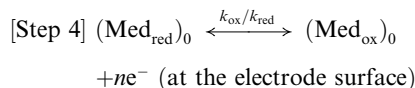
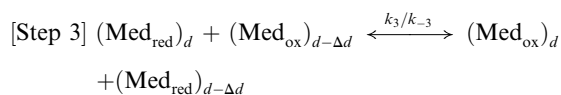
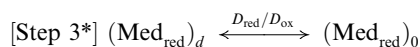
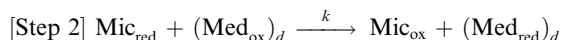
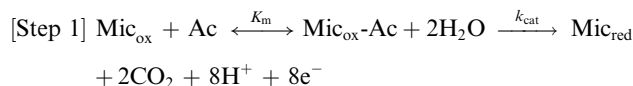


Fig. 1 Current-time records of current generation by WT *G. sulfurreducens* and deletion mutants during biofilm growth on graphite anodes. Self-determined thickness of each indicated where determined.

$\Delta omcE$, $\Delta omcST$, $\Delta omcZ$, and $\Delta pilA$), on equally-sized graphite fiber-based cloth anodes, in MFCs utilizing acetate as the electron donor and the anodes as the electron acceptors. Each biofilm, grown by connecting the anode to an oversized cathode through a resistor (not under potential or galvanic control), exhibited a growth pattern similar to that reported on anodes maintained at oxidizing potentials (e.g., +0.050 V to +0.300 V vs. SHE).^{32,36} Each biofilm grew to a self-determined thickness, indicated in Fig. 1. $\Delta omcB$, $\Delta omcE$, and $\Delta omcST$ each exhibited a growth rate and maximum catalytic current (*i*_d) similar to WT *G. sulfurreducens*. By contrast, $\Delta omcZ$ exhibited a previously described failed adaption³⁶ achieving a much lower unsustainable current and thickness after 10 days, and total loss of catalytic activity by 26 days. $\Delta pilA$ exhibited a previously described sustained current and thickness without adaption.^{17,32}

Cyclic voltammetry of wild type *G. sulfurreducens* biofilms

CV of the WT biofilms is anodic (positive current) and sigmoid-shaped at slow scan rate (Fig. 2 and 3A), and evolves into anodic and cathodic peaks at high scan rate (Fig. 4A). Such *i*-*E*-*v* dependencies are consistent with classic catalyst-dependent electrode reactions, first described in detail by Savéant and Vianello in 1965,⁵¹ and more recently by Katakis and Heller,⁵² to describe systems containing electrode-bound, non-diffusing, redox enzymes that couple oxidation of non-electrode-reactive substrates with reduction of electrode-reactive ET mediators. Following Katakis and Heller, we propose the reaction scheme below (depicted schematically in Fig. 5) for describing extracellular ET from microbes comprising an anode-bound biofilm of WT *G. sulfurreducens* to the anode surface. In this scheme, the biofilm is treated as a three-dimensional coating comprised of bound (*i.e.*, non-diffusing) catalysts reliant on ET mediators in the biofilm for transferring electrons through the biofilm and across the biofilm/electrode interface.



$$i = nFA(k_{\text{ox}}[(\text{Med}_{\text{red}})_0] - k_{\text{red}}[(\text{Med}_{\text{ox}})_0]) \quad (1)$$

Here, Mic_{ox} and Mic_{red} are oxidized and reduced microbes, Ac is acetate, and Med_{red} and Med_{ox} are reduced and oxidized forms of the ET mediator. In step 1, microbes with affinity for Ac of K_m oxidize Ac with rate constant k_{cat} , generating carbon dioxide and protons.⁵³ In step 2, each of the 8 electrons yielded by step 1

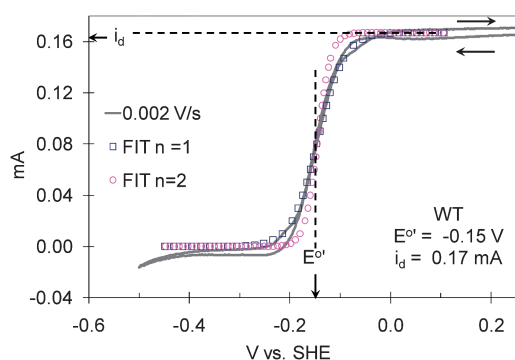


Fig. 2 Cyclic voltammetry of the *G. sulfurreducens* WT biofilm recorded at 0.002 V s^{-1} from 0.25 V to -0.50 V and back to 0.25 V vs. SHE qualitatively fitted to eqn (6) for $n = 1$ and $n = 2$, $i_d = 0.17 \pm 0.005 \text{ mA}$ and $E^{\circ'} = -0.145 \pm 0.01 \text{ V}$ vs. SHE.

undergo intracellular ET (resulting in the microbial metabolic benefit depicted in Fig. 5) and reduce Med_{ox} in the biofilm, at distance d from the anode surface regenerating Mic_{ox} with rate constant k . In step 3*, each $(\text{Med}_{\text{red}})_d$ diffuses into contact with the electrode ($d = 0$), with diffusion coefficient D_{red} . This ET mechanism is proposed for many non-corrosive biofilms investigated to date,⁵⁴ and relies on microbes secreting soluble (endogenous) ET mediators and/or utilizing naturally occurring or added (exogenous) mediators from the environment, e.g., *Geothrix*,⁵⁵ *Shewanella* (quinines^{56,57} and riboflavin^{39,58}) and *Pseudomonas* (Phenazines¹). If step 3* is reversible, Med_{ox} diffuses back through the biofilm for reuse by the microbes. Step 3 is an alternative mechanism for homogeneous ET we propose here for *G. sulfurreducens* based on results described below, in which the mediators are bound (non-diffusing) in the extracellular domain of the biofilm. Here, extracellular ET from distance

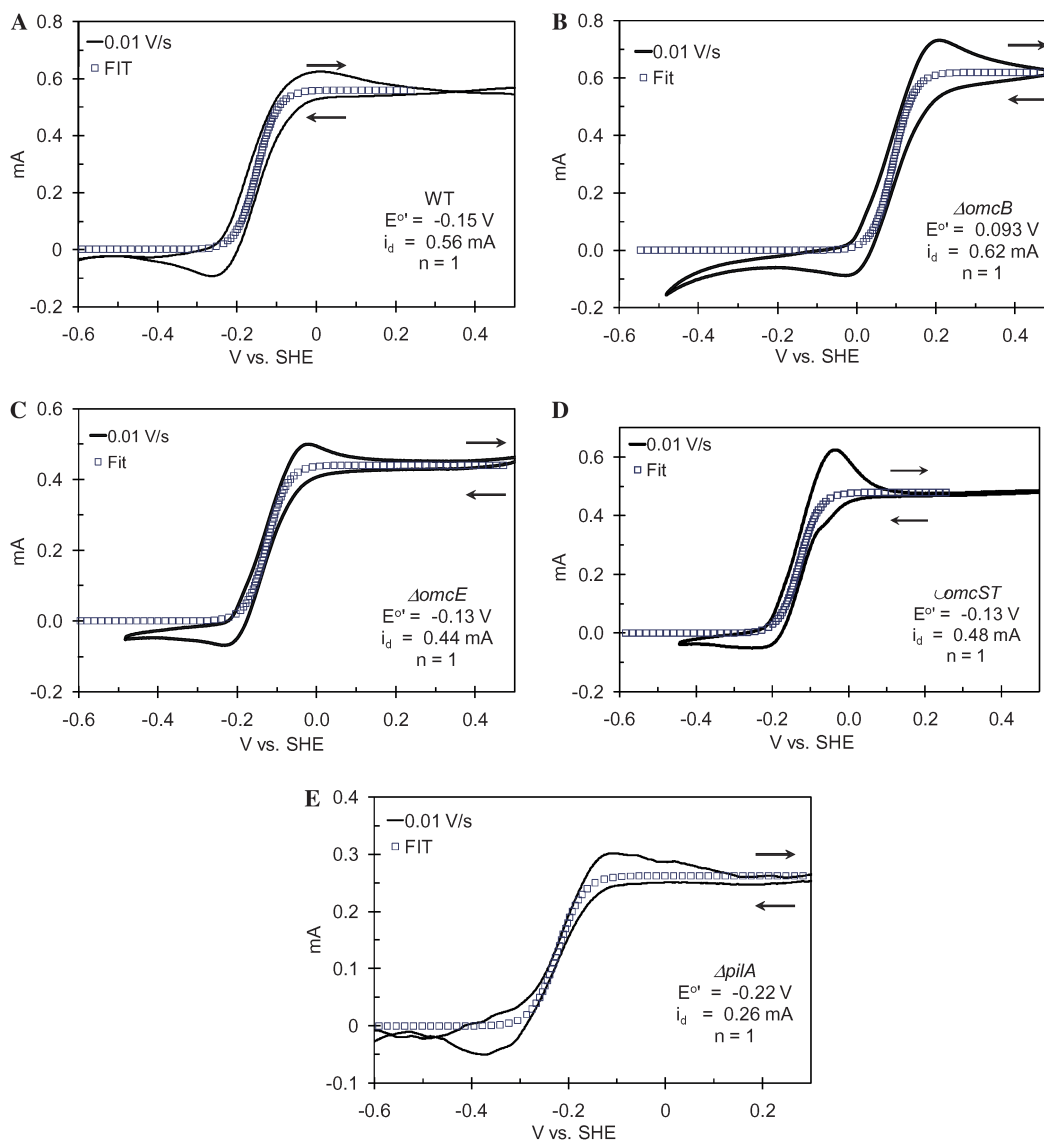


Fig. 3 CV recorded at 0.01 V s^{-1} from the indicated positive potential limit to the negative potential limit and back to the positive potential limit qualitatively fitted to eqn (6) of biofilms of A: WT *G. sulfurreducens*, B: ΔomcB ; C: ΔomcE ; D: ΔomcST ; E: ΔpilA .

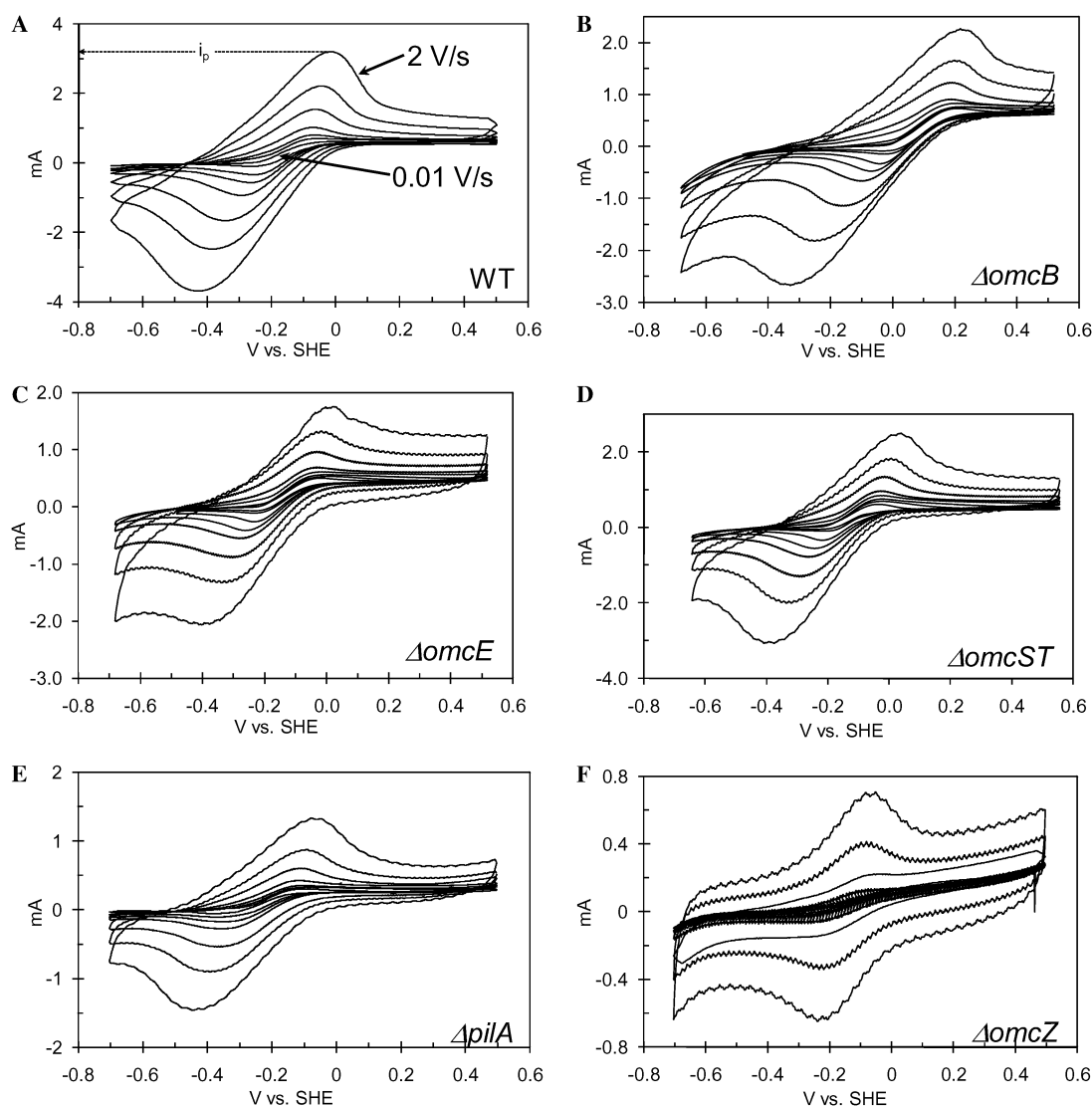


Fig. 4 Scan rate dependency of CV recorded from the indicated positive potential limit to the negative potential limit and back to the positive potential limit for biofilms of A: WT *G. sulfurreducens*; B: $\Delta omcB$; C: $\Delta omcE$; D: $\Delta omcST$; E: $\Delta pilA$; F: $\Delta omcZ$ recorded over a range of scan rates from 0.01 V s⁻¹ to 2 V s⁻¹. The anodic peak current (i_p) indicated for WT in case of 2 V s⁻¹.

d to the electrode surface occurs by a series of ET reactions among adjacent ET mediators with forward and reverse rate constants k_3 and k_{-3} . We model this mechanism on that proposed by Katakis and Heller⁵² for enzyme-modified electrodes, utilizing known bound ET mediators covalently attached within polymer films. In step 4 (heterogeneous ET), Med_{red} reduces the anode generating electrical current (i) across the biofilm–electrode interface (ne^- where n is the change in oxidation state of the ET mediator between the oxidized and reduced form), and regenerate Med_{ox} with forward and reverse rate constants k_{ox} and k_{red} . Eqn (1) relates current (i) resulting from step 4, where $[(Med_{red})_0]$ and $[(Med_{ox})_0]$ are concentrations of Med_{red} and Med_{ox} in immediate contact with the electrode surface, and A is the surface area of the electrode in cm². It is important to note that bound ET mediators require ion mobility to electrostatically balance the momentary change in oxidation state experienced by each individual ET mediator during each homogeneous and

heterogeneous ET event.^{59,60} Furthermore, distinct and multiple ET mediators may be involved in each step.¹³

In step 4, k_{ox} and k_{red} depend upon E as described by the Butler–Volmer electrode reaction rate expressions⁶¹

$$k_{ox} = k^0 \exp((1 - \alpha)(nF/RT)(E - E^0)) \quad (2)$$

$$k_{red} = k^0 \exp(-\alpha(nF/RT)(E - E^0)) \quad (3)$$

where E^0 is the formal potential of the ET mediator, k^0 is the standard rate constant for the heterogeneous ET step, α is the transfer coefficient,⁶¹ which ranges between 0 and 1 depending upon the specific electrode reaction, but typically takes the value of *ca.* 0.5, T is temperature (K), and R , T , and F are standard constants. Eqn (2) and (3) predict that when $E \gg E^0$, $k_{ox} \gg k^0 \gg k_{red}$; when $E = E^0$, $k^0 = k_{ox} = k_{red}$; and when $E \ll E^0$, $k_{ox} \ll k^0 \ll k_{red}$. If step 1 is fast (large k^0) compared to the scan

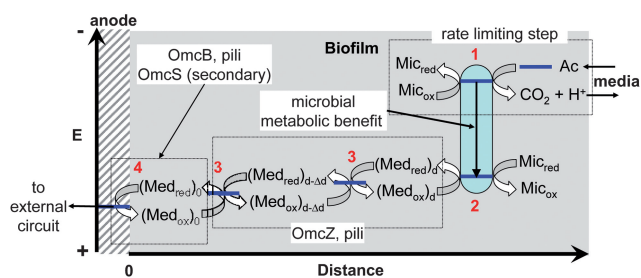


Fig. 5 Schematic depiction of electron transfer from acetate to the electrode surface catalyzed by a single microbe within a biofilm of WT *G. sulfurreducens*. Grey shaded area represents biofilm. The vertical axis indicates relative potential energy of electrons during electron transfer (as voltage increases, potential energy decreases). The horizontal axis indicates relative distance from the electrode surface. Red numbers indicate reaction step described in text. The reactant and product labels are defined in the text. Blue lines indicate relative potential energy of electrons at each step during electron transfer. The potential energy level of electrons at the anode surface is determined by the potentiostat during CV, directly affecting the kinetics and thermodynamics of step 4, which in turn affects the overall rate of electron transfer from acetate. The potential energy drop depicted to occur inside the microbe between acetate oxidation and mediator reduction is comprised, in part, by the metabolic benefit to the microbe. The potential energy drop depicted to occur through the biofilm results from a concentration gradient of reduced mediator caused by generation of reduced mediator by the microbe and consumption of reduced mediator at the anode. The relative energy levels are not drawn to scale.

rate (v , rate of change of E), $[(\text{Med}_{\text{ox}})_0]$ and $[(\text{Med}_{\text{red}})_0]$ will depend upon E as described by the Nernst equation.⁶¹

$$E = E^{\circ'} + RT/nF \ln([(Med_{\text{ox}})_0]/[(Med_{\text{red}})_0]) \quad (4)$$

If steps 3 or 3* are also fast (large k_3 and k_{-3} or D_{red} and D_{ox}) compared to the scan rate, $[\text{Med}_{\text{ox}}]$ and $[\text{Med}_{\text{red}}]$ (total concentrations of oxidized and reduced forms of the mediator in the biofilm) will also depend upon E as described by the Nernst equation in an analogous fashion. If in addition, step 2 is fast (large k) compared to the scan rate, catalytic current (i , eqn (1)) will scale linearly with $[\text{Med}_{\text{ox}}]$ up to the maximum catalytic current (i_d) because step 2 is first order with respect to $[\text{Med}_{\text{ox}}]$. This results in a sigmoid-shaped i - E dependency (e.g., Fig. 2) due to the sigmoid-shaped $[\text{Med}_{\text{ox}}]$ - E dependency expressed as:

$$[\text{Med}_{\text{ox}}] = [\text{Med}]/(1 + \exp((E^{\circ'} - E)(nF/RT))) \quad (5)$$

derived directly from the Nernst equation, where $[\text{Med}] = [\text{Med}_{\text{ox}}] + [\text{Med}_{\text{red}}]$ (the total concentration of ET mediator in the biofilm). Eqn (5) predicts that when $E \gg E^{\circ'}$, $[\text{Med}_{\text{ox}}] = [\text{Med}]$ (i.e., all ET mediator in the biofilm is oxidized) and maximum catalytic current (i_d) is observed. When $E = E^{\circ'}$ (the inflection point of Fig. 2), $[\text{Med}_{\text{ox}}] = [\text{Med}]/2$ (half as much current observed compared to when $[\text{Med}_{\text{ox}}] = [\text{Med}]$), and when $E \ll E^{\circ'}$, $[\text{Med}_{\text{ox}}] = 0$, and ideally no current is observed.

In Fig. 2, which was recorded during growth of the biofilm (i_d is therefore smaller compared to Fig. 1 at full growth), the experimental CV is qualitatively compared to the i - E dependency in eqn (6), derived directly from eqn (5).

$$(i_d - i)/i = \exp((E - E^{\circ'})(nF/RT)) \quad (6)$$

for $n = 1$ and $n = 2$, with $E^{\circ'} = -0.145\text{V vs. SHE}$ and $i_d = 0.167\text{ mA}$. Here, $E^{\circ'}$ is the formal potential of the mediator of the heterogeneous ET reaction (step 4), i is the catalytic current for a given E , and i_d is the maximum catalytic current at $E \gg E^{\circ'}$, when $[\text{Med}_{\text{ox}}]$ is at maximum value ($[\text{Med}]$). In turn, following classic enzyme kinetics, i_d can be expressed as:⁵³

$$i_d = nFAk_{\text{cat}}[\text{Mic}]/(1 + (k_{\text{cat}}/k[\text{Med}]) + (K_m)/[\text{Ac}]/8)) \quad (7)$$

where $[\text{Ac}]$ is the concentration of Ac in the biofilm (divided by 8 to account for the 8 electrons per equivalent of acetate oxidized), $[\text{Mic}]$ is the concentration of microbes in the biofilm, and A is the surface area of the electrode in cm^2 . The correlation (not rigorous) of Fig. 2 to eqn (6) for $n = 1$ and $E^{\circ'} = -0.145\text{ V vs. SHE}$ has the following implications: (1) Electrons are transferred through the biofilm by ET mediators one at a time (i.e., $n = 1$). (2) i scales proportionally with $[\text{Med}_{\text{ox}}]$ in response to the electrode potential (E). (3) i_d scales proportionally with $[\text{Med}]$. According to eqn (7), this would occur when $[\text{Ac}]/8 \gg K_m$ and $k_{\text{cat}} \gg k[\text{Med}]$, yielding eqn (8),

$$i_d = nFAk[\text{Mic}][\text{Med}] \quad (8)$$

indicating i_d is proportional to k , $[\text{Mic}]$ and $[\text{Med}]$ but limited by K_m (step 1). This outcome is consistent with our experience that i_d is independent of acetate concentration above 5 mM. (4) The biofilm is sufficiently conductive, such that its i - E dependency is not distorted by resistance (as exhibited by the *omcZ* deletion mutant described below). This conclusion is consistent with that of Bond *et al.* on the conductive nature of anode-bound biofilms of *G. sulfurreducens*³⁸ and with that of Torres *et al.*⁴⁶ on the conductive nature of anode-bound biofilms comprised predominantly of *G. sulfurreducens*.²⁸ (5) Heterogeneous ET (step 4) is sufficiently fast with respect to v (0.002 V s^{-1}) such that as E is changed, $[\text{Med}_{\text{ox}}]_0$ immediately adjusts to satisfy the Nernst equation. (6) Steps 3 or 3* are also sufficiently fast with respect to the scan rate, so that, as E changes, homogenous ET is sufficiently fast to satisfy the Nernst equation across the entire biofilm (i.e., $[\text{Med}_{\text{ox}}]_0 = [\text{Med}_{\text{ox}}]$). (7) The formal potential of the extracellular ET mediator in step 4 is $-0.15 \pm 0.01\text{ V vs. SHE}$, since it is the ET mediator (if others are acting in prior steps) the electrode reacts directly with. This value for $E^{\circ'}$ is in close agreement with that observed by Bond *et al.*⁷ and Schröder *et al.*¹ for *G. sulfurreducens* and with that of the *G. sulfurreducens* periplasmic cytochrome PpcA thought to donate electrons to outer membrane cytochromes in step 2 during iron reduction. It is important to note that correlation of Fig. 2 to eqn (6) does not require a homogenous population of microorganisms throughout the biofilm with respect to the rates of steps 1-4, only that for an overwhelming majority of microorganisms in the biofilm, steps 1-4 are very fast relative to the scan rate to ensure the appearance of a near overall Nernstian response (eqn (8)). It is also important to note that a small but non-negligible cathodic catalytic current is observed in Fig. 2 for $E < -0.2\text{ vs. SHE}$. The cause of this current is unknown at this time and we contend that it may result from *G. sulfurreducens* catalyzed reduction of trace components in the media.⁶² CVs (not shown) recorded in the

same media at bare graphite electrodes do not exhibit this reduction current.

Fig. 3A depicts the CV recorded at 0.010 V s^{-1} for a fully-grown biofilm of WT *G. sulfurreducens* (hence i_d in Fig. 3A is greater than observed in Fig. 2 and comparable to current observed at full growth in Fig. 1). While exhibiting the same formal potential and sigmoid-shape of Fig. 2, it also exhibits hysteresis and emergence of anodic and cathodic current peaks which become more pronounced with increasing scan rate (Fig. 4A). The cathodic scan in Fig. 3A (0.5 V to -0.6 V vs. SHE) corresponds to the lower current curve, while the anodic scan (-0.6 V back to 0.5 V vs. SHE) corresponds to the upper current curve. Hysteresis is typical of CV, and attributed here in small part to double-layer capacitance charging current which scales linearly with scan rate.⁶¹ It is attributed here to step 1 limiting catalytic current. During the cathodic scan, steps 3 and 4 accelerate in the reverse direction, as described by eqn (2) and (3), in order to satisfy the Nernst equation, and the electrode generates Med_{red} faster than the microbes can reduce remaining Med_{ox} (step 2). This results in the growing cathodic contribution (negative deviation) of the anodic current observed for $E \geq E^0$, and the cathodic peak is observed for $E \leq E^0$ when all remaining oxidized ET mediator is reduced by the electrode. Conversely, during the anodic scan, steps 3 and 4 accelerate in the forward direction, and the electrode generates Med_{ox} faster than the microbes can reduce it. This results in the growing anodic contribution (positive deviation) observed in the anodic current at $E \leq E^0$, and the anodic peak is observed for $E \geq E^0$ when all remaining Med_{ox} is oxidized by the electrode. The increasing anodic and cathodic peak currents recorded with increasing scan rate (Fig. 4A) result from systematically increasing the rate of acceleration of steps 3 and 4 beyond that encountered during generation of i_d (Fig. 2). The increasing peak splitting (potential of the anodic peak minus potential of the cathodic peak), observed with increasing scan rate (Fig. 4A), originates from the limitation in the rate of step 4, due to k^0 in eqn (2) and (3). In this qualitative description, we can not rule out heterogeneity among mediators throughout the biofilm with respect to the rates of steps 3 and 4 which would affect the peak shapes and dependency of peak splitting on scan rate.

Fig. 6A and B depict dependency with v and $v^{1/2}$ of the anodic peak currents (i_p), determined from Fig. 4A that are normalized by i_d determined at 0.010 V s^{-1} from Fig. 3A. These plots are based on that of Nicholson and Shain,⁶³ derived for catalyst-dependent electrode reactions, in which catalysts diffuse to the electrode surface. Their analysis indicated that i_p/i_d is expected to increase linearly with $v^{1/2}$, owing to the linear dependency of i_p vs. $v^{1/2}$ for non-catalyst-dependent electrode reactions in which a diffusing species is directly oxidized by an electrode.⁶¹ Here, i_p/i_d vs. v (Fig. 6A) is linear up to a threshold scan rate of 0.5 V s^{-1} . At faster scan rates i_p/i_d is linear with $v^{1/2}$ (Fig. 6B). This bimodal behavior, we contend, derives from confinement of ET mediators in biofilm, whether bound (insoluble) or unbound (soluble). Either condition is expected to result in linear i_p vs. v , at slow scan rates (if i_p is not limited by the rate of a diffusing species through the biofilm) in the case of either a soluble ET mediator (step 3*) or charge compensating ions (step 3).³² At faster scan rates there is less time for diffusion to occur; consequently, as step 3 or 3* is further accelerated, the linear i_p vs. $v^{1/2}$ dependency arises, when

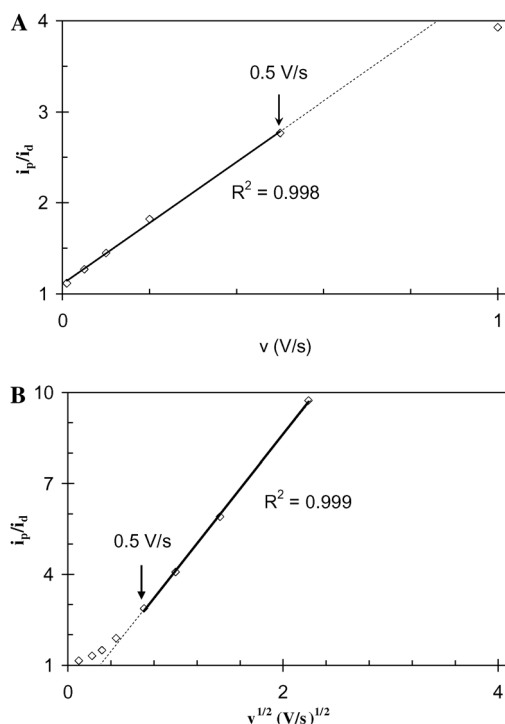


Fig. 6 For the WT *G. sulfurreducens* biofilm, A: Plot of anodic i_p/i_d vs. scan rate (v); B: plot of anodic i_p/i_d vs. $v^{1/2}$; both recorded in the presence of acetate.

current becomes limited by diffusion through the biofilm of either soluble ET mediator or charge compensating ions.⁶⁴ Fick's law of diffusion provides an estimation of the minimum diffusion coefficient (D) of the current-limiting soluble species for this transition to occur at 0.50 V s^{-1} ,⁶¹

$$D \gg L^2/(2t) \quad (9)$$

assuming L , the diffusion layer thickness, is the biofilm thickness (0.0002 cm). Here t is the time required to convert all ET mediator in the biofilm from the oxidized to reduced form at 0.50 V s^{-1} , which can be estimated from the width of the anodic peak base divided by scan rate ($0.80 \text{ V}/0.50 \text{ V s}^{-1} = 1.3 \text{ s}$), yielding $D \gg 1.5 \times 10^{-6} \text{ cm}^2 \text{ s}^{-1}$.

In contrast to Fig. 6A and B, Fig. 7B depicts a linear dependency of the anodic peak currents vs. $v^{1/2}$ for $v \ll 0.5 \text{ V s}^{-1}$, recorded in the absence of acetate, indicating that step 3 or 3* is more hindered by diffusion without acetate. Based on the recent results of Torres *et al.*,⁴⁶ we contend that the limitation in rate of homogenous ET, depicted in Fig. 6B at $v \geq 0.50 \text{ V s}^{-1}$ where the rate of homogenous ET is significantly accelerated beyond that required to maintain i_d , is due to diffusion of charge compensating protons (step 3). Charge compensation is more hindered in the absence of acetate since protons are generated inside the biofilm by step 1. The minimum diffusion coefficient determined above is low compared to that of protons in water ($9.3 \times 10^{-5} \text{ cm}^2 \text{ s}^{-1}$)⁶⁴ or even in a (hypothetical) dense biofilm ($9.3 \times 10^{-6} \text{ cm}^2 \text{ s}^{-1}$)^{65,66} and is consistent with proton diffusion being limited in turn by buffer diffusion at the biofilm/media interface.⁶⁶

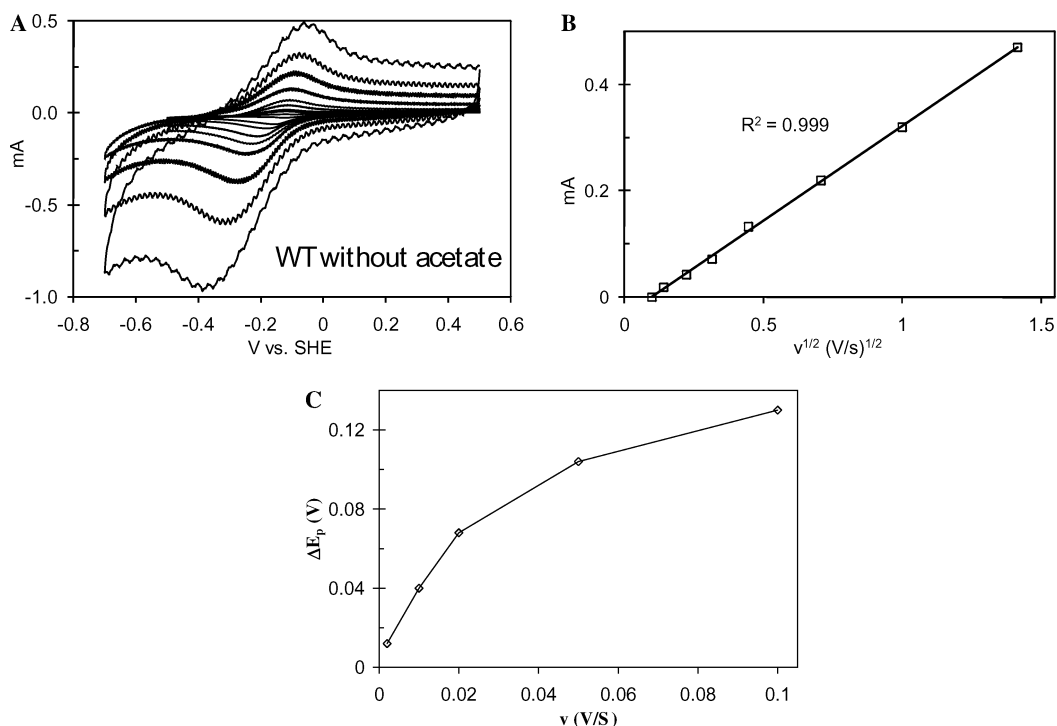


Fig. 7 For the WT *G. sulfurreducens* biofilm, A: CV recorded from the indicated positive potential limit to the negative potential limit to the positive potential limit over a range of scan rates from 0.01 V s⁻¹ to 2 V s⁻¹ in the absence of acetate; B: Plot of i vs. $v^{1/2}$.

It is recognized that the above treatment is qualitative and not rigorous because microorganisms are not individual enzymes, nor were the voltammograms fitted to simulations of steps 1–4 to yield values for various reaction parameters including the degree of possible heterogeneity among the microbes and mediators in the biofilm (work in progress), it does provide however, a useful model for studying the mechanism of extracellular ET in the *Geobacter sulfurreducens* biofilms.

Cyclic voltammetry of $\Delta omcB$, $\Delta omcE$, $\Delta omcST$, and $\Delta pilA$ biofilms

As with the wild type biofilms, CVs recorded at a moderately slow scan rate (0.010 V s⁻¹) for $\Delta omcB$, $\Delta omcE$, $\Delta omcST$, and $\Delta pilA$ mutant biofilms (Fig. 3) can be qualitatively fitted to eqn (6) taking into account the above described hysteresis and emergence of peaks which are more pronounced at faster scan rates (Fig. 6). The conclusions drawn from Fig. 3 about the wild type biofilm therefore apply to these mutant biofilms, as well; they are conductive, rapidly exchange electrons with electrodes, and are limited in current generation by step 1. There are significant differences, however, among E^0 values of *omcB* (+0.090 V) and $\Delta pilA$ (-0.22 V) compared to WT *G. sulfurreducens* (-0.15 V), indicating that OmcB and pili are important in the heterogeneous ET reaction (step 4). In the case of $\Delta pilA$, E^0 is shifted significantly negative (Fig. 3E). As depicted in Fig. 5, this increases potential energy of electrons transferred to the anode, possibly decreasing the metabolic benefit to this mutant, since E^0 of ET mediators involved in steps 2 and 3 (if different from ET mediators involved in step 4) may also need to shift negative in order to enable homogenous ET. The $\Delta pilA$ biofilm is, however,

conductive (as evidenced by the sigmoid-shape of its 0.010 V s⁻¹ CV compared to $\Delta omcZ$ described below), but thin compared to the WT *G. sulfurreducens* biofilm (6 vs. 20 μm). The maximum catalytic current is ca. 50% that of the WT biofilm, or ca. 1.5 fold higher when normalized by thickness. A decreased metabolic benefit may be consistent with the necessity to produce more current per individual cell for viability. These results suggest that pili may not be directly involved in the homogenous ET (step 3), owing to conductivity of the $\Delta pilA$ biofilm, but that pili may play a structural role in formation of thick biofilms and in localization of extracellular *c*-type cytochromes,⁶⁷ contributing to step 4 (hence causing the shift in E^0).

Unlike $\Delta pilA$, E^0 of the $\Delta omcB$ biofilm is shifted significantly positive, to +0.09 V vs. SHE (Fig. 3B). As depicted in Fig. 5, this could decrease potential energy of electrons transferred to the anode. This shift in formal potential indicates that OmcB is most likely the mediator responsible for heterogeneous ET (step 4) in WT *G. sulfurreducens*. This outcome is supported by the results of Nevin *et al.*,³⁶ who determined that OmcB is over expressed in thick high-current producing biofilms, and by Franks *et al.*,⁶⁸ demonstrating that this induction is specifically localized at the innermost layer (cells closest to the anode surface) of the biofilm. Since the $\Delta omcB$ biofilm achieves the same growth rate and maximum catalytic current as the WT biofilm, and does not require additional time to adapt, we contend that the $\Delta omcB$ mutant likely utilizes the same homogeneous ET mediator in step 3 as WT, and an alternative ET mediator in step 4, present *a priori* in WT *G. sulfurreducens*, with a much more positive E^0 that is not viable for Fe(III) oxide reduction.²⁶

Unlike $\Delta omcB$, the $\Delta omcE$ and $\Delta omcST$ (Fig. 3C and D) exhibit E^0 values (-0.13 V vs. SHE) relatively similar to E^0 of

WT *G. sulfurreducens*. Both exhibit the same growth rate and maximum catalytic current as WT *G. sulfurreducens* (Fig. 1), but $\Delta omcST$ undergoes an extended lag phase before producing current (Fig. 1). These results suggest that OmcE is not directly involved in step 4, in spite of being necessary for Fe(III) oxide reduction.¹⁸ In contrast, OmcS appears to be involved in steps 2 and/or 3 as indicated by impaired Fe(III) oxide reduction by $\Delta omcST$ ¹⁸ and by the extended lag-phase required for anode reduction (Fig. 1). We contend that during the lag phase an adaptation occurs resulting in expression of an alternative mediator not involved in step 4. (OmcT was not been evaluated separately since its abundance on the surface of WT cells is negligible and Fe(III) oxide reduction can be restored in $\Delta omcST$ by complementation with *omcS* alone, but not with *omcT*.⁵)

Cyclic voltammetry of $\Delta omcZ$ biofilms

CVs of $\Delta omcZ$ (Fig. 8 recorded at maximum growth current = 0.25 mA) are markedly different from those of WT *G. sulfurreducens* and the other mutant strains. There is a pronounced resistive dependency (linear $i-v$ feature) superimposed onto the sigmoid dependency described above. Such an $i-v$ dependency is often observed for electrode-bound redox enzymes (non-diffusing). It occurs if the enzyme exchanges electrons directly with an electrode surface (heterogeneous ET) without relying on ET mediators, there is a distribution in the rate of heterogeneous ET due to a distribution among individual enzymes in orientation to electrode surface, and if a substantial portion of the enzyme population possesses relatively slow (*i.e.*, resistive)

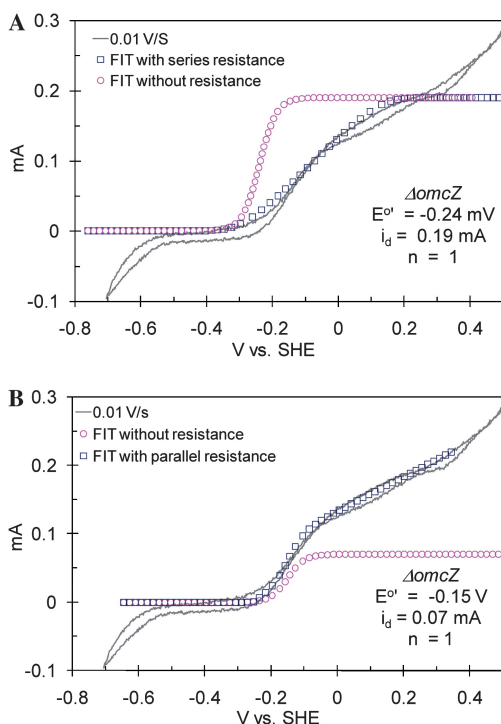


Fig. 8 CV recorded at 0.01 V s⁻¹ from 0.45 V to -0.7 V and back to 0.45 V vs. SHE of a $\Delta omcZ$ biofilm, fitted as (A): uniform biofilm in which all microbes encounter resistive ET paths to the electrode surface and (B): 2-component biofilm in which one component encounters conductive ET paths, the other resistive ET paths.

heterogeneous ET rates compared to the scan rate.⁶⁹ Two strategies for analyzing the $\Delta omcZ$ CVs were evaluated. In the first (Fig. 8A), it was assumed that all microbes comprising the biofilm encountered resistive extracellular ET pathways, either due to step 3 or 4 being slow. The experimental current was roughly fit to eqn (6), assuming $E^{\circ} = -0.24$ V vs. SHE and $i_d = 0.19$ mA; then resistance was added in series to suppress this current and better fit the experimental data. Here i_d was chosen to match the inflection observed in the experimental data at *ca.* 0.0 V vs. SHE, once resistance was added. This approach to fitting the experimental data requires a very negative E° , regardless of the resistance used. In the second approach (Fig. 8B) we assumed a two-component biofilm comprised of a population of microbes with relatively conductive extracellular ET pathways to the anode (presumably those in direct contact with the anode) and a population of microbes with resistive extracellular ET pathways to the anode (presumably not in direct contact with the anode). In this approach the experimental data was first fit to eqn (6), assuming $E^{\circ} = -0.15$ V vs. SHE and $i_d = 0.07$ mA, and then resistance added in parallel to augment this current and better fit the experimental data. Here, i_d was also chosen to match the inflection observed in the experimental data at *ca.* 0.0 V vs. SHE, once resistance was added to yield a unique solution for E° (-0.150 V vs. SHE). This value for E° is consistent with E° exhibited by this biofilm at fast scan rates (Fig. 4F), which can be approximated by averaging the potentials of the anodic and cathodic peaks (-0.145 ± 0.01 V vs. SHE, at 0.10 V s⁻¹) and better fits the current at $E > 0.2$ V vs. SHE. This suggests that the two-component biofilm hypothesis more accurately describes the biofilm of the OmcZ-deficient mutant, in which i_d (0.07 mA) is attributed to current generation by microbes with more conductive extracellular ET pathways not affected by deletion of *omcZ* since E° is the same as for WT. Deletion of *omcZ*, therefore, appears to significantly impair the rate of step 3 for a significant portion of the microbes in the biofilm indicating its potential role in mediating the homogenous ET reaction. The anodic and cathodic peaks observed at faster scan rates (Fig. 4F) would therefore be attributed to reduction and oxidation of mediator contributing to step 1 for the microbes with the conductive extracellular ET pathways.

Conclusion

The CV of the electrode-bound biofilm of WT *Geobacter sulfurreducens* depicted here is remarkably similar to that of electrode-bound non-diffusing redox enzymes developed by Heller *et al.*^{52,65}. Based on this similarity, we propose a multi-step reaction scheme for extracellular ET from individual microorganisms comprising the biofilm to the underlying anode surface. We interpreted the wild type CV based on this model, and compared it to CV of anode-bound biofilms of mutant strains deficient in various *c*-type cytochromes or the PilA protein. Our results indicate that WT *G. sulfurreducens* forms a conductive network of bound ET mediators that most likely utilizes OmcZ to transfer electrons through the biofilm and OmcB to transfer electrons across the electrode/biofilm interface; that pili are important in both reactions, that OmcS and T are of secondary importance to the former, and that OmcE is not involved in extracellular ET during anode reduction in spite of being

necessary for Fe(III) oxide reduction. In the case of Heller's electrode immobilized redox enzymes,^{52,65} co-immobilized organometallic complex's that are covalently attached within a porous polymer matrix by flexible linkers transfer electrons from the enzymes (analogous to step 2), among themselves (analogous to step 3), and with the electrode surface (analogous to step 4) through a series of thermally activated collisions. In the case of *G. sulfurreducens*, homogenous ET may be occurring between individual OmcZ proteins along a cell's outer membrane and by cell-to-cell contact toward the electrode surface where OmcB on the innermost microbes to the anode surface mediate the heterogeneous electron transfer reaction. By analogy to Heller's electrode immobilized enzymes, homogeneous electron transfer from individual microbes comprising the biofilm may be driven thermodynamically by a concentration gradient of reduced mediator in which reduced mediator is generated by the microbes and consumed by the anode.^{70,71} Our analysis also indicates that the magnitude of catalytic current is limited by rate of acetate uptake by the microbes. Furthermore, the homogeneous electron transfer process (step 3), when accelerated during fast scan CV, becomes limited by diffusion of protons in the biofilm generated by oxidation of acetate (step 1), which serve as charge compensating counter ions in the homogenous ET. This analysis provides a useful model to advance strategies to increase the power density of microbial fuel cells.

Acknowledgements

We are grateful to helpful discussions with Professor Daniel Bond. This research was supported by the Office of Naval Research Award No. N00014-07-1-0996 and N00014-07-WX20515 and by Office of Science (BER), U. S. Department of Energy, Cooperative Agreement No. DE-FC02-02ER63446.

References

- 1 B. E. Logan, B. Hamelers, R. Rozendal, U. Schröder, J. Keller, S. Freguia, P. Alterman, W. Verstraete and K. Rabaey, *Environ. Sci. Technol.*, 2006, **40**, 5181.
- 2 D. R. Lovley, *Nat. Rev. Microbiol.*, 2006, **4**, 497–508.
- 3 L. M. Tender, S. A. Gray, E. Groveman, D. A. Lowy, P. Kauffman, J. Melhado, R. C. Tyce, D. Flynn, R. Petrecca and J. Dobarro, *J. Power Sources*, 2008, **179**, 571–575.
- 4 A. K. Shukla, P. Suresh, S. Berchmans and A. Rajjendran, *Curr. Sci.*, 2004, **87**, 455–468.
- 5 Z. Du, H. Li and T. Gu, *Biotechnol. Adv.*, 2007, **25**, 464–482.
- 6 D. R. Bond, D. E. Holmes, L. M. Tender and D. R. Lovley, *Science*, 2002, **295**, 483–5.
- 7 L. M. Tender, C. E. Reimers, H. A. Stecher, D. E. Holmes, D. R. Bond, D. A. Lowy, K. Pilobello, S. J. Fertig and D. R. Lovley, *Nat. Biotechnol.*, 2002, **20**, 821–825.
- 8 D. E. Holmes, D. R. Bond, R. A. O'Neil, C. E. Reimers, L. M. Tender and D. R. Lovley, *Microb. Ecol.*, 2004, **48**, 178–190.
- 9 S. Jung and J. M. Regan, *Appl. Microbiol. Biotechnol.*, 2007, **77**, 393–402.
- 10 H. S. Lee, P. Parameswaran, A. Kato-Marcus, C. I. Torres and B. E. Rittmann, *Water Res.*, 2008, **42**, 1501–1510.
- 11 S. Ishii, K. Wantanabe, S. Yabuki, B. E. Logan and Y. Sekiguchi, *Appl. Environ. Microbiol.*, 2008, in press.
- 12 Y. Liu, F. Harnisch, K. Fricke, R. Sietmann and U. Schröder, *Biosens. Bioelectron.*, 2008, in press.
- 13 K. Fricke, F. Harnisch and U. Schröder, *Energy Environ. Sci.*, 2008, **1**, 144–147.
- 14 D. R. Bond and D. R. Lovley, *Appl. Environ. Microbiol.*, 2003, **69**, 1548–1555.

- 15 K. P. Nevin, S. F. Covalla, J. P. Johnson, T. L. Woodard, H. Jia, M. Zhang and D. R. Lovley, *Environ. Microbiol.*, 2008, in press.
- 16 D. E. Holmes, S. K. Chaudhuri, K. P. Nevin, T. Mehta, B. A. Methe, A. Liu, J. E. Ward, T. L. Woodard, J. Webster and D. R. Lovley, *Environ. Microbiol.*, 2006, **8**, 1805–1815.
- 17 G. Reguera, K. D. McCarthy, T. Mehta, J. S. Nicoll, M. T. Tuominen and D. R. Lovley, *Nature*, 2005, **435**, 1098–1101.
- 18 T. Mehta, M. V. Coppi, S. E. Childers and D. R. Lovley, *Appl. Environ. Microbiol.*, 2005, **71**, 8634–8641.
- 19 E. Afkar, G. Reguera, M. Schiffer and D. R. Lovley, *BMC Microbiol.*, 2005, **5**, 41.
- 20 J. E. Butler, F. Kaufmann, M. V. Coppi, C. Nunez and D. R. Lovley, *J. Bacteriol.*, 2004, **186**, 4042–4045.
- 21 A. Esteve-Núñez, C. Núñez and D. R. Lovley, *J. Bacteriol.*, 2004, **186**, 2897–2899.
- 22 A. Esteve-Nunez, J. Sosnik, P. Visconti and D. R. Lovley, *Environ. Microbiol.*, 2008, **10**, 497–505.
- 23 K. B. Gregory, D. R. Bond and D. R. Lovley, *Environ. Microbiol.*, 2004, **6**, 596–604.
- 24 B. C. Kim, D. Leang, Y. R. Ding, R. H. Glaven, M. V. Coppi and D. R. Lovley, *J. Bacteriol.*, 2005, **187**, 4505–13.
- 25 B. C. Kim, X. L. Qian, C. Leang, M. V. Coppi and D. R. Lovley, *J. Bacteriol.*, 2006, **188**, 3138–3142.
- 26 C. Leang, M. V. Coppi and D. R. Lovley, *J. Bacteriol.*, 2003, **185**, 2096–2103.
- 27 C. Leang and D. R. Lovley, *Microbiol.*, 2005, **151**, 1761–1767.
- 28 C. Leang, L. A. Adams, K. J. Chin, K. P. Nevin, K. B. A. Methé, J. Webster, M. L. Sharma and D. R. Lovley, *J. Bacteriol.*, 2005, **187**, 5918–5926.
- 29 J. R. Lloyd, C. Leang, A. L. Hodeges-Myerson, M. V. Coppi, S. Cuifo, B. Methe, S. J. Sandler and D. R. Lovley, *Biochem. J.*, 2003, **369**, 153–161.
- 30 T. Mehta, S. E. Childers, R. Glaven, D. R. Lovley and T. Mester, *Microbiol.*, 2006, **152**, 2257–64.
- 31 X. Qian, G. Reguera, T. Mester and D. R. Lovley, *FEMS Microbiol. Lett.*, 2007, **277**, 21–27.
- 32 G. Reguera, K. P. Nevin, J. S. Nicoll, S. F. Covalla, T. L. Woodard and D. R. Lovley, *Appl. Environ. Microbiol.*, 2006, **72**, 7345–7348.
- 33 G. Reguera, R. B. Pollina, J. S. Nicoll and D. R. Lovley, *J. Bacteriol.*, 2007, **189**, 2125–2127.
- 34 H. Richter, K. D. McCarthy, K. P. Nevin, J. P. Johnson, V. M. Rotello and D. R. Lovley, *Langmuir*, 2008, **24**, 4376–4379.
- 35 E. S. Shelobolina, M. V. Coppi, A. A. Korenevsky, L. N. DiDonato, S. A. Sullivan, H. Konishi, H. Xu, C. Leang, J. E. Butler, B. C. Kim and D. R. Lovley, *BMC Microbiol.*, 2007, **7**, 16.
- 36 K. P. Nevin, B. C. Kim, R. H. Glaven, J. P. Johnson, T. L. Woodard, B. A. Methé, R. J. DiDonato Jr, S. F. Covalla, A. E. Franks, A. Liu and D. R. Lovley, *J. Bacteriol.*, 2008, submitted.
- 37 B. C. Kim, K. P. Nevin and D. R. Lovley, ASM General Meeting, 2008, Poster Q-386.
- 38 S. Srikanth, E. Marsili, M. C. Flickinger and D. R. Bond, *Biotechnol. Bioeng.*, 2007, **99**, 1065–1073.
- 39 E. Marsili, D. B. Baron, I. D. Shikhare, C. Coursolle, J. A. Gralnick and D. R. Bond, *Proc. Natl. Acad. Sci. U. S. A.*, 2008, **105**, 3968–3973.
- 40 M. Lanthier, K. B. Gregory and D. R. Lovley, *FEMS Microbiol. Lett.*, 2007, **278**, 29–35.
- 41 D. P. Lies, M. E. Hernandez, A. Kappler, R. E. Mielke, J. A. Gralnick and D. K. Newman, *Appl. Environ. Microbiol.*, 2005, **71**, 4414–4426.
- 42 A. Price-Whelan, L. E. P. Dietrich and D. K. Newman, *J. Bacteriol.*, 2007, **189**, 6372–6381.
- 43 S. S. Ruebush, S. Brantley and M. Tien, *Appl. Environ. Microbiol.*, 2006, **72**, 2925–2935.
- 44 K. M. Rosso, J. M. Zachara, J. K. Fredrickson, Y. A. Gorby and S. C. Smith, *Geochim. Cosmochim. Acta*, 2003, **67**, 1081–1087.
- 45 K. P. Nevin and D. R. Lovley, *Appl. Environ. Microbiol.*, 2000, **66**, 2248–2251.
- 46 C. I. Torres, A. Kato Marcus and B. E. Rittmann, *Biotechnol. Bioeng.*, 2008, **100**, 872–881.
- 47 F. Caccavo, D. J. Lonergan, D. R. Lovley, M. Davis, J. F. Stolz and M. J. McInerney, *Appl. Environ. Microbiol.*, 1994, **60**, 3752–3759.
- 48 M. V. Coppi, C. Leang, S. J. Sandler and D. R. Lovley, *Appl. Environ. Microbiol.*, 2001, **67**, 3180–3187.
- 49 D. R. Lovley and E. J. P. Phillips, *Appl. Environ. Microbiol.*, 1988, **54**, 1472–1480.

-
- 50 A. M. Bond, K. B. Oldham and G. A. Snook, *Anal. Chem.*, 2000, **72**, 3492–3496.
- 51 J. M. Savéant and E. Vianello, *Electrochim. Acta*, 1965, **10**(10), 905–920.
- 52 I. Katakis and A. Heller, *Anal. Chem.*, 1992, **64**, 1008–1013.
- 53 J. Hodak, R. Etchenique and E. J. Calvo, *Langmuir*, 1997, **13**(10), 2708–2716.
- 54 M. E. Hernandez and D. K. Newman, *Cell. Mol. Life Sci.*, 2001, **58**, 1562–1571.
- 55 D. R. Bond and D. R. Lovley, *Appl. Environ. Microbiol.*, 2005, **71**, 2186–9.
- 56 D. K. Newman and R. A. Kolter, *Nature*, 2000, **405**, 93–97.
- 57 D. P. Lies, M. E. Hernandez, A. Kappler, R. E. Mielke, J. A. Gralnick and D. K. Newman, *Appl. Environ. Microbiol.*, 2005, **71**, 4414–4426.
- 58 H. V. Canstein, J. Ogawa, S. Shimizu and J. R. Lloyd, *Appl. Environ. Microbiol.*, 2008, **74**(3), 615–623.
- 59 T. R. Brumleve and R. P. Buck, *J. Electroanal. Chem.*, 1981, **126**, 105–119.
- 60 R. P. Buck and C. Mundt, *Electrochim. Acta*, 1999, **44**(12), 1999–2018.
- 61 A. J. Bard and L. R. Faulkner, *Electrochemical Methods*, John Wiley & Sons, Inc, 2nd edn, 2001.
- 62 K. B. Gregory and D. R. Lovley, *Environ. Sci. Technol.*, 2005, **39**, 8943–8947.
- 63 R. S. Nicholson and I. Shain, *Anal. Chem.*, 1964, **36**(4), 706–723.
- 64 R. J. Forster, D. A. Walsh, N. Mano, F. Mao and A. Heller, *Langmuir*, 2004, **20**(3), 862–868.
- 65 S. Mudliar, S. Banerjee, A. Vaidya and S. Devotta, *Bioresour. Technol.*, 2008, **99**, 3468–3474.
- 66 H. Horn and E. Morgenroth, *Chem. Eng. Sci.*, 2006, **61**, 1347–1356.
- 67 M. Izallalen, R. H. Glaven, T. Mester, K. P. Nevin, A. E. Franks and D. R. Lovley, *ASM General Meeting*, 2008, poster I-034.
- 68 A. E. Franks, K. P. Nevin, A. L. Orloff, M. Izallalen, D. Keymeulen, D. K. Newman and D. R. Lovley, *ASM General Meeting*, 2008, poster Q-391.
- 69 C. Leéger and P. Bertrand, *Chem. Rev.*, 2008, **108**(7), 2379–2438.
- 70 F. B. Kaufman and M. B. Engler, *J. Am. Chem. Soc.*, 1979, **101**, 547.
- 71 F. B. Kaufman, A. M. Schroeder, E. M. Engler, S. R. Kramer and J. Q. Chambers, *J. Am. Chem. Soc.*, 1980, **102**, 483.